Transient-state operation of an anoxic biotrickling filter for H_2S removal

Ramita Khanongnuch[a*], Francesco Di Capua[c], Aino-Maija Lakaniemi[a], Eldon R. Rene[b], Piet N. L. Lens[a, b]

[a]Tampere University, Faculty of Engineering and Natural Sciences, P. O. Box 541, 33014 Tampere, Finland

[b]UNESCO-IHE Institute for Water Education, P.O. Box 3015, 2601 DA Delft, The Netherlands

[c]Department of Civil, Architectural and Environmental Engineering, University of Naples Federico II, 80125 Naples, Italy

[*]Corresponding author:

Ramita Khanongnuch

Tampere University, Faculty of Engineering and Natural Sciences, P. O. Box 541, 33014 Tampere, Finland

E-mail: ramita.khanongnuch@tuni.fi

Abstract

The application of an anoxic biotrickling filter (BTF) for H_2S removal from contaminated gas streams is a promising technology for simultaneous H_2S and NO_3^- removal. Three transient-state conditions, i.e. different liquid flow rates, wet-dry bed operations and H_2S shock loads, were applied to a laboratory-scale anoxic BTF. In addition, bioaugmentation of the BTF with a H_2S removing-strain, *Paracoccus* MAL 1HM19, to enhance the biomass stability was investigated. Liquid flow rates (120, 60 and 30 L d^{-1}) affected the pH and NO_3^- removal efficiency (RE) in the liquid phase. Wet-dry bed operations at 2-2 h and 24-24 h reduced the H_2S elimination capacity (EC) by 60-80%, while the operations at 1-1 h and 12-12 h had a lower effect on the BTF performance. When the BTF was subjected to H_2S shock loads by instantly increasing the gas flow rate (from 60 to 200 L h^{-1}) and H_2S inlet concentration (from 112 ± 15 to 947 ± 151 ppm_v), the BTF still showed a good H_2S RE (>93%, EC of 37.8 g S m^{-3} h^{-1}). Bioaugmentation with *Paracoccus* MAL 1HM19 enhanced the oxidation of the accumulated S^0 to sulfate in the anoxic BTF.

Keywords: H_2S removal; biotrickling filter; wet-dry bed operations; transient loading; PCR-DGGE

1. Introduction

Hydrogen sulfide (H_2S) is one of the major gaseous pollutants emitted from anaerobic digesters, landfill sites, and petroleum refining processes and the H_2S concentration can be as high as 10,000 ppm_v [1,2]. H_2S can cause an immediate hazard to human health at concentrations >600 ppm_v [3]. Biogas utilization as a fuel in internal combustion engines should contain H_2S levels <100 ppm_v, while biogas application in gas stoves and fuel cells requires even lower H_2S concentrations (<10 ppm_v) [4]. Among the different biological techniques for H_2S removal from waste-gas streams, biotrickling filters (BTFs) are widely used because they are easy to operate, economically viable and more efficient than conventional biofilters [5]. The major difference is that the trickling liquid in the BTF is continuously passed over the filter bed (packed with inert materials) to provide sufficient moisture and nutrients for the growth of microorganisms present in the BTF.

In recent years, H_2S removal in anoxic BTFs using nitrate (NO_3^-) as an electron acceptor has gained increasing interest [6–9]. Anoxic H_2S removal is carried out by sulfur-oxidizing nitrate-reducing (SO-NR) bacteria, according to Eqs. (1) and (2) [10]:

$$HS^- + 1.23NO_3^- + 0.093NH_4^+ + 0.438HCO_3^- + 0.573H^+ + 0.027CO_2 \rightarrow 0.093C_5H_7O_2N + 0.614N_2 + SO_4^{2-} + 0.866H_2O \quad (1)$$

$$HS^- + 0.350NO_3^- + 0.013NH_4^+ + 0.059HCO_3^- + 1.4H^+ + 0.004CO_2 \rightarrow 0.013C_5H_7O_2N + 0.175N_2 + S^0 + 1.21H_2O \quad (2)$$

During full-scale BTF operation, unexpected (transient) operating conditions, such as a process shut down during weekends, equipment malfunctions, sudden or unexpected changes in process conditions, are regularly encountered and can cause irregular inlet gas flow rates and variations in the inlet contaminant concentrations. This will affect the activity of microorganisms as well as the bioreactor stability [11,12]. Furthermore, in full-scale BTF, intermittent trickling liquid supply may be applied as an operational strategy to minimize

pressure drop and operational costs [13,14]. Thus, the effect of different trickling liquid supply (wet-dry operations) on the anoxic BTF performance requires further investigation.

Recent studies have investigated the impact of transient conditions, such as pollutant shock loads and starvation periods, on the performance of aerobic BTFs removing H_2S and other gaseous pollutants [15–19]. In the literature, anoxic BTFs have been studied using different packing materials, H_2S loading rates, gas or liquid flow rates and using automated control strategies (i.e. feedback and feedforward control) [8,20–23]. However, the impact of different H_2S shock loads on the H_2S and NO_3^- removal and microbial community composition has not yet been investigated. Moreover, the study of bioaugmentation with SO-NR bacteria is interesting to enhance the biomass stability of an anoxic BTF for simultaneous removal of H_2S and NO_3^-.

The present study aimed, therefore, to evaluate the response of an anoxic BTF to: (i) different liquid flow rates, (ii) wet-dry bed operations, and (iii) H_2S shock loads by suddenly increasing both the gas flow rate and the inlet H_2S concentration in the gas stream. Furthermore, bioaugmentation of the BTF with a biomass dominated by *Paracoccus* MAL 1HM19 was performed.

2. Materials and methods

2.1. BTF set-up and trickling liquid composition

The anoxic BTF used in this study (Fig. S1) was previously operated for 138 d under steady-state conditions [24]. The BTF, having an inner diameter and height of 12 and 50 cm, respectively, was packed with polyurethane foam (PUF) cubes (8 cm^3 each, total volume 2.11 L) as described by Khanongnuch et al. [24]. The trickling liquid consisted of a NO_3^--rich medium containing (per 1 L): 0.07-0.46 g KNO_3, 1 g $NaHCO_3$, 0.2 g KH_2PO_4, 0.1 g NH_4Cl, 0.08 g $MgSO_4 \cdot 7H_2O$, 1 mL $FeSO_4 \cdot 7H_2O$ solution (2 mg L^{-1}) and 0.2 mL of trace element solution, as described by Khanongnuch et al. [24]. The pH of the medium was adjusted to

~7.0 with 37% HCl. The inlet gas stream consisted of a mixture of N_2 and synthetic H_2S as described by Khanongnuch et al. [24].

2.2. BTF operation

The BTF was operated for 78 days to evaluate three different transient-state conditions (phases I-III) and investigate the bioaugmentation of the BTF (phase IV) (Fig. S2). Table 1 describes the operational conditions tested during each transient-state test and normal operation. The normal operation was applied for 1-4 days to stabilize the BTF performance at the end of each transient-state test to achieve complete recovery of the H_2S RE to >98%. The tricking liquid flow rate was 60 L d^{-1} and the actual hydraulic retention time of NO_3^--rich medium was 19 min [24]. The trickling liquid was composed of fresh NO_3^--containing medium and reactor effluent, being fed to the BTF at a flow rate ratio of 1:5. According to Eq. 1, the theoretical N/S ratio for complete H_2S oxidation is 1.23. During the entire study, the feed NO_3^- was supplied in excess (27.8 ± 1.2 mg L^{-1}) to the BTF, corresponding to a feed nitrogen-sulfur (N/S) molar ratio of 3.0, to ensure the complete H_2S oxidation. During phases I, II and III, the effect of, respectively, the liquid flow rates, wet-dry bed operation and H_2S shock load conditions was tested. In phase IV, the BTF was bioaugmented with a biomass dominated by *Paracoccus* MAL 1HM19 which is a SO-NR bacterium isolated from a hot spring in Thailand showing good capacity to grow at varied environmental conditions, e.g. NaCl concentrations of 0.03-7% *w/v* and temperatures of 20-50 °C [25].

Table 1.

During phase I (days 0-19), the BTF was operated under liquid flow rates increasing stepwise from 30 to 60 and 120 L d^{-1}, corresponding to a trickling liquid velocity (TLV) of 0.1 to 0.2 and 0.4 m h^{-1}, respectively. On days 20-21, the BTF was stabilized before initiating the next transient condition.

During phase II (days 22-50), the BTF was tested under four different wet-dry bed operations by supplying the trickling liquid to the BTF at four different time intervals: (i) 12 h wet-12 h dry (days 22-30), (ii) 24 h wet-24 h dry (days 31-41), (iii) 1 h wet-1 h dry (days 42-45) and (iv) 2 h wet-2 h dry (days 46-50). The liquid flow rate was controlled using an automatic timer to switch the peristaltic pumps on or off.

During phase III (days 51-62), H_2S shock loads were tested by suddenly increasing (i) the gas flow rate (days 51-55) and (ii) the inlet H_2S concentration (days 56-62). Each shock load was applied for 4 h and repeated for a duplicate test after 24 h of the first shock load (Table 1). First, the gas flow rate was instantly increased from 60 to 200 L h^{-1} while maintaining the inlet H_2S concentration constant at 115 (±18) ppm_v, resulting in an increase of the H_2S loading rate from 4.4 (±0.8) to 14.0 (±1.5) g S m^{-3} h^{-1} (days 51-55). Then, the inlet H_2S concentration was increased from 112 (±15) to 947 (±151) ppm_v at a constant gas flow rate of 60 L h^{-1}, resulting in an increase of the H_2S loading rate from 4.2 (±0.6) to 35.5 (±5.6) g S m^{-3} h^{-1} (days 56-62).

On day 63 (phase IV), the BTF was bioaugmented with PUF cubes obtained from another laboratory-scale anoxic BTF dominated by a facultative autotrophic denitrifying bacterium, *Paracoccus* MAL 1HM19 [25]. One third of the PUF cubes (88 pieces) in the BTF of the present study were removed and replaced with PUF cubes of the other BTF containing *Paracoccus* MAL 1HM19. From day 70 onwards, the response of the BTF to H_2S shock loads of the bioaugmented BTF was tested. In this test, the inlet H_2S concentration was increased from 110 (±13) to 982 (±70) ppm_v for 4 h and repeated for a duplicate test at 24 h after the first shock load (Table 1). The parameters used to evaluate the BTF performance and the equations used to calculate these parameters are given in the supplementary material.

2.3. Analytical techniques

The influent and effluent pH was measured using a Präzision pH Meter (Metrohm, Switzerland) equipped with a SenTix 21 pH electrode (WTW, Germany). Liquid samples of the BTF influent and effluent were measured for total dissolved sulfide (HS^- and S^{2-}) and NO_2^- concentrations using colorimetric methods [26] with a Lamda 365 UV/VIS spectrophotometer (Perkin-Elmer, USA). The liquid samples were filtered through 0.45 µm cellulose acetate syringe filters (Sigma-Aldrich, USA) prior to the measurements of NO_3^-, $S_2O_3^{2-}$ and SO_4^{2-} concentrations by ion chromatography performed as described by Villa-Gomez et al. [27]. The volatile suspended solids (VSS) of the BTF effluent were determined according to the procedure given in Standard Methods [26]. A Dräger X-am® 7000 gas detector (Dräger, Germany) with a detection range of 0-500 ppm_v and a Geotech Biogas-5000 gas analyzer (Hatech Gasdetectietechniek BV, The Netherlands) with a detection range of 500-5000 ppm_v were used to measure the inlet and outlet H_2S concentrations of the BTF.

The statistical differences in the performance parameters among each phase of the BTF operation, e.g. EC and RE, were determined using Tukey's multiple comparison tests (a one-way ANOVA, Minitab Inc., USA). Data sets were compared and considered significantly different when *p-value* ≤ 0.05 was obtained.

2.4. Microbial community analysis

Two pieces of randomly selected PUF cubes were collected from the BTF on days 0, 62 and 78. DNA was extracted using the DNeasy® PowerSoil® Kit (QIAGEN, Germany), followed by polymerase chain reaction (PCR) and denaturing gradient gel electrophoresis (DGGE), as described by Khanongnuch et al. [28]. The DNA sequencing was performed by Marcrogen (The Netherlands). The obtained sequences were analyzed using the BioEdit software (version 7.2.5) and compared with sequences from the National Center for

Biotechnology Information (NCBI) database (https://blast.ncbi.nlm.nih.gov) using the BLASTn search tool.

3. Results

3.1. Effect of trickling liquid velocity

At different TLV (0.1, 0.2 and 0.4 m h^{-1}) (phase I), the H_2S RE of the BTF was constant at 100% and corresponded to a H_2S EC of 3.7 (±0.3) g S m^{-3} h^{-1}. A partial oxidation of H_2S to S^0 likely occurred at TLV of 0.1 m h^{-1}, as the produced SO_4^{2-} (136 ± 49 mg S d^{-1}) with respect to the removed H_2S was 84 (±12)% (Fig. 1c, days 0-6). At this TLV, the consumed N/S ratio was 1.1 (±0.1) mol mol^{-1} which was significantly lower than the values at 0.2 and 0.4 m h^{-1} (~2.0 mol mol^{-1}) (*p-value* ≤0.000).

The increase TLV from 0.1 to 0.2 and 0.4 m h^{-1}, corresponding to an increase of the NO_3^- loading rate from 2.7 (±0.1) to 5.2 (±0.3) and 11.3 (±0.5) g NO_3^--N m^{-3} h^{-1}, resulted in an increase of the NO_3^- removal rate from 1.4 (±0.1) to 2.3 (±0.3) and 2.6 (±0.6) g NO_3^--N m^{-3} h^{-1}, respectively (Fig. 1b). However, the increase in TLV from 0.1 to 0.2 and 0.4 m h^{-1} resulted in a decrease of the effluent pH from 8.3 (±0.1) to 8.0 (±0.1) and 7.7 (±0.1), respectively (Fig. 1d) (*p-value* ≤0.000).

Fig. 1.

3.2. Effect of wet-dry bed operations

During 12 h wet-12 h dry operation, the NO_3^--containing liquid phase was fed to the BTF for 12 h, at an interval of 24 h from days 22-30 (Fig. 2a). During days 24-30, the H_2S RE decreased from 100 to 87% after 6-h of dry operation (Fig. 2b). The NO_3^- RE fluctuated in the range of 32.0-56.8% during days 22-23, whereas a stable NO_3^- RE (45.9 ± 3.0%) was observed from day 25 onwards (Fig. 2c).

Fig. 2.

During 24 h wet-24 h dry operation, the BTF was fed with the trickling liquid for 24 h at an interval of 48 h from days 31-41 (Fig. 3a). During this test, the H_2S RE decreased from 100% to 35.6% (day 35) after 24 h of dry operation; however, the H_2S RE recovered to 100% within 3.5 h after resuming the trickling liquid supply (Fig. 3b). At the end of the 24 h wet-24 h dry operation, the H_2S RE showed a longer recovery time, as complete H_2S removal was observed after 84 h of resuming the normal operating conditions (day 40). The NO_3^- RE ranged between 42.2 and 61.6% during this test (days 31-41) (Fig. 3c). The S^0 previously accumulated in the BTF was likely oxidized during this feeding regime, resulting in the SO_4^{2-}-S production of 105%-404% (Fig. 3b). During the entire study, other sulfur species, i.e. S^{2-} and $S_2O_3^{2-}$, were not observed in the effluent.

Fig. 3.

During 1 h wet-1 h dry operation (days 42-43), the H_2S RE was relatively stable in the range of 84.3-98.3% (Fig. 4b) and the H_2S RE was still >98% when the BTF was operated under normal conditions (days 44-45). During 2 h wet-2 h dry operation, the H_2S RE decreased to 75.0% during days 46-47 and thereafter to 56.7% during days 47-48. At the end of the wet-dry operation, the H_2S RE recovered to 98.3% after the trickling liquid had been continuously fed to the BTF for ~62 h (day 50) which was shorter than the 24 h wet-24 h dry operation. The NO_3^- RE was 39.3 (±3.8)% and 42.4 (±3.6)% during 1 h wet-1 h dry and 2 h wet-2 h dry operations, respectively (Fig. 4c).

Fig. 4.

During the entire wet-dry operation tests, the consumed N/S ratio was similar in the range of 1.3-1-5 (*p-value* ≤0.215). The H_2S EC values during 12 h wet-12 h dry and 1 h wet-1 h dry operations were similar (3.8 and 3.9 g S m^{-3} h^{-1}, respectively) and close to the 100% performance line (Fig. 5a). The 24 h wet-24 h dry and 2 h wet-2 h dry operations resulted in lower H_2S EC (3.3 and 3.5 g S m^{-3} h^{-1}, respectively) (*p-value* ≤0.000).

Fig. 5.

3.3. Effect of H_2S shock loads

The sudden increase in the gas flow rate from 60 to 200 L h^{-1} increased the H_2S loading rate from 4.4 to 14.0 g S m^{-3} h^{-1}, while the EBRT reduced from 3 to 0.9 min. On day 51, the highest H_2S EC was 13.1 g S m^{-3} h^{-1} (Fig. 5b), while the H_2S RE was 96.9 (±1.1)% and decreased to the lowest value of 72.0%. However, the H_2S RE recovered to 96.0 (±1.1)% within 16 h when the gas flow rate was restored to 60 L h^{-1} (Fig. 6a, days 53-55). Besides, SO_4^{2-}-S was mainly produced during this test (120 ± 40)% (Fig. 6b, days 50-62).

During the subsequent H_2S shock load tests by increasing inlet H_2S from 110 (±13) to 982 (±70) ppm_v, the H_2S RE decreased to its lowest value of 68.9% (day 57). The maximum H_2S EC was 37.8 g S m^{-3} h^{-1} (H_2S RE of 93.9%) (Fig. 5b). The sudden increase of the H_2S concentration resulted in partial H_2S oxidation to S^0 due to NO_3^- limitation because the consumed N/S ratio was ~0.22 (Fig. S2f) and the SO_4^{2-}-S production was <20% (Fig. 6b). After each peak of shock loads, the consumed N/S ratio gradually increased from 1.3 (±0.4) on day 51 to 2.1 (±0.3) on day 60 (*p-value* ≤0.004), corresponding to the increase of NO_3^- RE from 40.4% to 56.0%, respectively (Fig. 6c). After this H_2S shock load test, when the inlet H_2S concentration was decreased to 116 (±2) ppm_v, the H_2S RE recovered from the lowest value of 73.6% (days 60) to >98.0% within 40 h (Fig. 6a).

Fig. 6.

3.4. Bioaugmentation with Paracoccus MAL 1HM19

After the BTF was bioaugmented with *Paracoccus* MAL 1HM19 (days 63-68), the H_2S RE was 96.8 (±2.1)% (Fig. 7a), corresponding to a H_2S EC of 4.49 (±0.19) g S m^{-3} h^{-1} (Fig. 7b). The bioaugmentation increased the NO_3^- RE from 46.3 (±1.2)% (phase III, days 50-61) to 80.4 (±5.0)% (phase IV, days 63-68), corresponding to an increase in the NO_3^- removal rate from 2.6 (±0.3) to 4.5 (±0.2) g NO_3^--N m^{-3} h^{-1} (Fig. 7b). The consumed N/S ratio was 1.5

(±0.4) mol mol^{-1} prior to the bioaugmentation, which increased to 9.9 (±3.6) mol mol^{-1} after subjecting the bioaugmented BTF to a H_2S shock load (Fig. S1f, days 74-78).

Fig. 7.

When a H_2S shock load was applied to the bioaugmented BTF (days 70-71), the H_2S RE sharply decreased from 96.9 (±0.6)% to 12.0% (day 70) and 34.4% (day 71) after applying the first and second shock loads for 5.0 h and 4.3 h, respectively (Fig. 7a). The SO_4^{2-} production rate gradually increased from 219 mg S d^{-1} (day 70) to 669 mg S d^{-1} (day 74). During days 71-73, the H_2S RE did not completely recover after the H_2S shock loads and fluctuated in the range of 34.4-70.6%. On day 74, when the influent NO_3^- concentration was increased from 27.8 (±1.2) to 84.0 (±0.6) mg L^{-1}, the H_2S RE increased to >98% (Fig. 7a, days 75-78). Besides, the NO_3^- RE was 87.1 (±9.1)% (Fig. 7c, days 74-78), corresponding to a NO_3^- removal rate of 14.4 (±1.4) g NO_3^--N m^{-3} h^{-1}. The increase in SO_4^{2-} production rate (713 mg S d^{-1}) on day 75 corresponded to a ~300% increased SO_4^{2-}-S production based on 190 mg H_2S-S d^{-1} removed (Fig. 7b).

3.5. Microbial community composition in the BTF

The microbial community composition visualized by DGGE showed an increase in the number of individual bands after the transient-state tests (day 62) and the bioaugmentation (day 78) of the BTF (Fig. 8). During all operational conditions, bacteria identified as *Thiobacillus* sp. (bands 5, 7 and 8), *Rhodobacter* sp. (bands 2 and 15), *Stenotrophomonas* sp. (bands 1 and 11), *Rhodocyclales* bacterium (band 5) and bacteria belonging to *Bactroidetes* (bands 3 and 4) were detected (Fig. 8). The bacteria with >99% similarity to the endosymbiont of *Acanthamoeba* sp. (band 14) and *Geobacter* sp. (band 16) were present after finishing the transient-state tests (day 62). After the bioaugmentation with *Paracoccus* MAL 1HM19 (day 78), DGGE bands of bacteria identified as *Paracoccus* sp. (bands 10 and 13) and *Simplicispira* sp. (band 9) were present in the BTF, while the band related to *Thiobacillus*

sp. (band 5) and *Stenotrophomonas* sp. (band 11) had a lower intensity compared to days 0 and 62.

Fig. 8.

4. Discussion

4.1. BTF response to changes in liquid flow rate

The increase in TLV (0.1-0.4 m h^{-1}) did not significantly affect the H_2S RE of the BTF (Fig. 1c). Similarly, previous observations in BTFs reported that the liquid flow rate only slightly affected the removal of gas-phase pollutants at low concentrations, especially when the pollutants are water soluble [23,29]. Subjecting the BTF to a high liquid flow rate could, nevertheless, reduce the biofilm stability and generate increased shear stress causing biofilm to wash out from the system [29]. In this study, the low biomass concentration in the effluent (VSS <30 mg L^{-1}) suggested that no biofilm sloughing had occurred.

At the lowest TLV tested (0.1 m h^{-1}), partial oxidation of H_2S to S^0 using NO_3^- as electron acceptor likely occurred, as 84 (±12)% of the consumed H_2S was converted to SO_4^{2-} (Fig. 1c), although sufficient NO_3^- was supplied to the BTF (feed N/S ratio of 1.7 ± 0.2). However, the consumed N/S ratio was 1.2 (±0.1), which causes the partial H_2S oxidation to S^0 in typical anoxic BTFs [8,23,30]. In contrast, the higher TLV tested in the BTF, i.e. 0.2 and 0.4 m h^{-1}, increased the %SO_4^{2-}-S production to 122 (±24)% (Fig. 1c). This indicated that sufficient NO_3^- concentration was supplied to the sulfide-oxidizing biofilm in the BTF when the TLV was higher than 0.1 m h^{-1}. However, the TLV of 0.4 m h^{-1} likely provided an overload of the NO_3^- to the anoxic BTF (11.3 ± 0.5 g NO_3^--N m^{-3} h^{-1}), as the NO_3^- removal rate was only <3.3 (±0.6) g NO_3^--N m^{-3} h^{-1} resulting in a NO_3^- RE of 32 (±7)% (Fig. 1b, days 7-20). Besides, an increase in the liquid flow rate in the BTF decreased the NO_3^- retention time in the anoxic BTF causing NO_3^- breakthrough in the effluent as evidenced by the lower consumed N/S ratio at the TLV of 0.4 m h^{-1} compared to the N/S ratio at 0.2 m h^{-1} (Fig. 1b).

The anoxic BTF in this study was operated at low TLVs (0.1-0.4 m h^{-1}) compared to previous studies [9,31]. However, our study showed that the low TLVs applied were effective for the treatment of H_2S and NO_3^- concentrations as high as ~1000 ppm_v and ~30 mg L^{-1}, respectively.

4.2. Effect of intermittent flow of the trickling liquid

The anoxic BTF showed a high resilience capacity to tolerate gas-phase H_2S (88-147 ppm_v) in the absence of the trickling liquid and NO_3^- for 24 h. During 24 h wet-24 h dry operation, the H_2S RE recovered to 100% immediately after resuming the liquid recirculation despite the severe reduction of H_2S RE observed during the dry operation (Figs. 2 and 3). It has been shown previously that autotrophic bacteria can tolerate inorganic carbon and nutrient starvation during dry-bed operation [32]. Heterotrophic and mixotrophic bacteria can also survive by degrading easily biodegradable biofilm components (i.e. extracellular polymeric substances) or organic compounds excreted by autotrophic bacteria [33].

The 12 h wet-12 h dry and 1 h wet-1 h dry operations resulted in high and stable BTF performance, with similar H_2S EC values (Fig. 5a). However, the lowest average NO_3^- RE during the 1 h wet-1 h dry operation (39.3%, Fig. 4c) might have caused S^0 accumulation during long-term operation. This observation also suggests that the 1 h duration caused a too short pulse feeding and led to poor liquid distribution through the packed bed. While the reduction of the NO_3^- RE was not observed during the 2 h wet-2 h dry operation, the H_2S EC showed a high fluctuation (Fig. 5a). Those short pulse feeding regimes (1 h and 2 h) were detrimental to the H_2S RE, which significantly decreased during the operation (Fig. 4b).

In further studies, residence time distribution (RTD) tests should be performed to obtain a better understanding of the effects of different modes of wet-dry operations on the hydrodynamic behavior of anoxic BTF and their effects on microbial activity.

4.3. Resistance of the BTF to intermittent H_2S loads

The anoxic BTF showed a faster recovery time compared to those reported for an aerobic biofilter treating H_2S (loading rate of 1-6 g H_2S m^{-3} h^{-1}), which was subjected to a H_2S shock load of 10 g H_2S m^{-3} h^{-1} [19]. Kim et al. [19] showed that the recovery time to attain the H_2S RE of ~100% after restoring the initial H_2S load was 96 h. Jing et al. [34] tested sulfide shock loads by applying (for 2 h) 1.5-3 times higher inlet concentrations (520 mg S^{2-}-S L^{-1}) in an anaerobic upflow bioreactor treating sulfide and NO_3^- in synthetic wastewater. The authors reported that the recovery time was 30 h at the highest tested concentration (1820 mg S^{2-}-S L^{-1}), which was similar to the recovery time observed in our study when the BTF was subjected to a 10-fold increase in the H_2S loading rate (Fig. 6a). The H_2S RE improved during the succeeding H_2S shock loads, resulting in a higher H_2S RE than when the first shock load was applied (Fig. 6a). This suggests that the microorganisms adapted to the intermittent H_2S loading regime in the anoxic BTF.

López et al. [35] successfully used a feedforward control in the anoxic BTF to reduce the impact of H_2S load disturbances (28-141 g S m^{-3} h^{-1}). Although the H_2S loads used in their study were much higher than the values of this study, the consumed N/S ratio during the H_2S load disturbance was similar (~0.2-2.1 mol mol^{-1}). Furthermore, our study revealed that the NO_3^- requirement for the BTF gradually increased after the shock loads as NO_3^- was likely used to oxidize the S^0 accumulated as a product of partial H_2S oxidation. This suggests that the NO_3^- in the influent should be provided in excess if the BTF is expected to receive H_2S shock loads during its long-term operation.

4.4. Microbial community composition

The DGGE profiles of the microbial community in the BTF after the transient-state tests, i.e. different liquid flow rates, H_2S shock loads and wet-dry operations, were slightly different than those of the initial biomass (Fig. 8). Surprisingly, the microbial community was

enriched with the endosymbiont of *Acanthamoeba* sp. and *Geobacter* sp., which likely do not play roles in sulfide oxidation [36–38]. It should be noted, however, that those bacteria might not be viable as they have a lower intensity at the end of the BTF operation (day 78) (Fig. 8). This study showed the stability of microbial community composition in the anoxic BTF to withstand different transients-state conditions, resulting in a stable H_2S EC (4.0 ± 0.2 g S m^{-3} h^{-1}) at the end of experiment (days 75-78).

Bioaugmentation of the BTF with *Paracoccus* MAL 1HM19 did not affect the H_2S EC but increased ~2 times of NO_3^- removal compared to the value prior to bioaugmentation. The bioaugmentation, followed by the H_2S shock load, stimulated the utilization of NO_3^- as electron acceptor to oxidize the previously accumulated S^0 in the BTF (Eq. 2), resulting in a high SO_4^{2-}-S production (~300%) at the end of the experiment (days 74-78). To develop the BTF for simultaneous treating of H_2S-contaminated gas streams and wastewater containing NO_3^- and COD, mixotrophic or heterotrophic denitrification could be stimulated in the BTF by e.g. bioaugmentation with *Paracoccus* MAL 1HM19. The heterotrophic bacteria enable to utilize various organic carbon sources (e.g. acetate, glucose and pyruvate) during anoxic H_2S oxidation [25].

5. Conclusions

H_2S shock loads up to 35.5 (±5.6) g S m^{-3} h^{-1} only slightly affected the BTF performance, resulting in the highest EC of 37.8 g S m^{-3} h^{-1} with >93% H_2S RE. Modification of the BTF liquid supply, i.e. TLV and wet-dry bed operation, should be taken into account in designing and operating anoxic BTFs to avoid the depletion of the electron acceptor and mass transfer limitations. Bioaugmentation with biomass dominated with the SO-NR bacterium, *Paracoccus* MAL 1HM19, revealed the feasibility of H_2S removal at high NO_3^- loading rates. Considering its good resiliency and resistance to various transient-state conditions, anoxic

BTFs are an attractive option in full-scale applications combining waste-gas clean-up (H_2S removal) with wastewater treatment (NO_3^- removal).

6. Acknowledgements

This work was supported by the European Union's Horizon 2020 research and innovation programme [grant number 643071] under the Marie Skłodowska-Curie European Joint Doctorate (EJD) *Advanced Biological Waste-To-Energy Technologies* (ABWET).

7. References

[1] Z. Yang, J. Liu, J. Cao, D. Sheng, T. Cai, J. Li, A comparative study of pilot-scale bio-trickling filters with counter- and cross-current flow patterns in the treatment of emissions from chemical fibre wastewater treatment plant, Bioresour. Technol. 243 (2017) 78–84. doi:10.1016/j.biortech.2017.06.060.

[2] R. Muñoz, L. Meier, I. Diaz, D. Jeison, A review on the state-of-the-art of physical/chemical and biological technologies for biogas upgrading, Rev. Environ. Sci. Biotechnol. 14 (2015) 727–759. doi:10.1007/s11157-015-9379-1.

[3] C. Yalamanchili, M.D. Smith, Acute hydrogen sulfide toxicity due to sewer gas exposure, Am. J. Emerg. Med. 26 (2008) 7–9. doi:10.1016/j.ajem.2007.08.025.

[4] S.K. Khanal, Y. Li, Biogas Production and Applications, in: Y. Li, S.K. Khanal (Eds.), Bioenergy Principles and Applications, John Wiley & Sons, Inc., New York, 2017, pp. 338–360.

[5] K. Barbusinski, K. Kalemba, D. Kasperczyk, K. Urbaniec, V. Kozik, Biological methods for odor treatment – A review, J. Clean. Prod. 152 (2017) 223–241. doi:10.1016/j.jclepro.2017.03.093.

[6] M. Ben Jaber, A. Couvert, A. Amrane, P. Le Cloirec, E. Dumont, Hydrogen sulfide removal from a biogas mimic by biofiltration under anoxic conditions, J. Environ. Chem. Eng. 5 (2017) 5617–5623. doi:10.1016/j.jece.2017.10.029.

[7] J.C. López, E. Porca, G. Collins, R. Pérez, A. Rodríguez-Alija, R. Muñoz, G. Quijano, Biogas-based denitrification in a biotrickling filter: Influence of nitrate concentration and hydrogen sulfide, Biotechnol. Bioeng. 114 (2017) 665–673. doi:10.1002/bit.26092.

[8] M. Fernández, M. Ramírez, J.M. Gómez, D. Cantero, Biogas biodesulfurization in an anoxic biotrickling filter packed with open-pore polyurethane foam, J. Hazard. Mater. 264 (2014) 529–535. doi:10.1016/j.jhazmat.2013.10.046.

[9] F. Almenglo, M. Ramírez, J.M. Gómez, D. Cantero, Operational conditions for start-up and nitrate-feeding in an anoxic biotrickling filtration process at pilot scale, Chem. Eng. J. 285 (2016) 83–91. doi:10.1016/j.cej.2015.09.094.

[10] M. Mora, M. Fernández, J.M. Gómez, D. Cantero, J. Lafuente, X. Gamisans, D. Gabriel, Kinetic and stoichiometric characterization of anoxic sulfide oxidation by SO-NR mixed cultures from anoxic biotrickling filters, Appl. Microbiol. Biotechnol. 99 (2014) 77–87. doi:10.1007/s00253-014-5688-5.

[11] G. Rodriguez, A.D. Dorado, M. Fortuny, D. Gabriel, X. Gamisans, Biotrickling filters for biogas sweetening: Oxygen transfer improvement for a reliable operation, Process Saf. Environ. Prot. 92 (2014) 261–268. doi:10.1016/j.psep.2013.02.002.

[12] P. San-Valero, C. Gabaldón, J.M. Penya-roja, G. Quijano, Enhanced styrene removal in a two-phase partitioning bioreactor operated as a biotrickling filter: Towards full-scale applications, Chem. Eng. J. 309 (2017) 588–595. doi:10.1016/j.cej.2016.10.054.

[13] F. Sempere, C. Gabaldón, V. Martínez-Soria, P. Marzal, J.M. Penya-roja, F. Javier Álvarez-Hornos, Performance evaluation of a biotrickling filter treating a mixture of oxygenated VOCs during intermittent loading, Chemosphere. 73 (2008) 1533–1539. doi:10.1016/j.chemosphere.2008.08.037.

[14] Deshusses, M.A., Gabriel, D., 2005. Biotrickling Filter Technology, in: Shareefdeen,

Z., Singh, A. (Eds.), Biotechnology for Odor and Air Pollution Control. Springer-Verlag Berlin Heidelberg, Germany, pp. 147–168. https://doi.org/10.1007/b138434.

[15] B.T. Mohammad, E.R. Rene, M.C. Veiga, C. Kennes, Performance of a thermophilic gas-phase biofilter treating high BTEX loads under steady- and transient-state operation, Int. Biodeterior. Biodegrad. 119 (2017) 289–298. doi:10.1016/j.ibiod.2016.10.054.

[16] M.E. López, E.R. Rene, Z. Boger, M.C. Veiga, C. Kennes, Modelling the removal of volatile pollutants under transient conditions in a two-stage bioreactor using artificial neural networks, J. Hazard. Mater. 324 (2017) 100–109. doi:10.1016/j.jhazmat.2016.03.018.

[17] E.R. Rene, M.E. López, M.C. Veiga, C. Kennes, Steady- and transient-state operation of a two-stage bioreactor for the treatment of a gaseous mixture of hydrogen sulphide, methanol and α-pinene, J. Chem. Technol. Biotechnol. 85 (2010) 336–348. doi:10.1002/jctb.2343.

[18] A.C. Romero Hernandez, M.S. Rodríguez Susa, Y. Andrès, E. Dumont, Steady-and transient-state H_2S biofiltration using expanded schist as packing material, N. Biotechnol. 30 (2013) 210–218. doi:10.1016/j.nbt.2012.07.003.

[19] J.H. Kim, E.R. Rene, H.S. Park, Biological oxidation of hydrogen sulfide under steady and transient state conditions in an immobilized cell biofilter, Bioresour. Technol. 99 (2008) 583–588. doi:10.1016/j.biortech.2006.12.028.

[20] G. Soreanu, M. Béland, P. Falletta, B. Ventresca, P. Seto, Evaluation of different packing media for anoxic H_2S control in biogas, Environ. Technol. 30 (2009) 1249–1259. doi:10.1080/09593330902998314.

[21] A.M. Montebello, M. Fernández, F. Almenglo, M. Ramírez, D. Cantero, M. Baeza, D. Gabriel, Simultaneous methylmercaptan and hydrogen sulfide removal in the

desulfurization of biogas in aerobic and anoxic biotrickling filters, Chem. Eng. J. 200–202 (2012) 237–246. doi:10.1016/j.cej.2012.06.043.

[22] F. Almenglo, T. Bezerra, J. Lafuente, D. Gabriel, M. Ramírez, D. Cantero, Effect of gas-liquid flow pattern and microbial diversity analysis of a pilot-scale biotrickling filter for anoxic biogas desulfurization, Chemosphere. 157 (2016) 215–223. doi:10.1016/j.chemosphere.2016.05.016.

[23] M. Fernández, M. Ramírez, R.M. Pérez, J.M. Gómez, D. Cantero, Hydrogen sulphide removal from biogas by an anoxic biotrickling filter packed with Pall rings, Chem. Eng. J. 225 (2013) 456–463. doi:10.1016/j.cej.2013.04.020.

[24] R. Khanongnuch, F. Di Capua, A.-M. Lakaniemi, E.R. Rene, P.N.L. Lens, H_2S removal and microbial community composition in an anoxic biotrickling filter under autotrophic and mixotrophic conditions, J. Hazard. Mater. 367 (2018) 397–406. doi: 10.1016/j.jhazmat.2018.12.062

[25] W. Watsuntorn, C. Ruangchainikom, E.R. Rene, P.N.L. Lens, W. Chulalaksananukul, Hydrogen sulfide oxidation under anoxic conditions by a nitrate-reducing, sulfide-oxidizing bacterium isolated from the Mae Um Long Luang hot spring, Thailand, Int. Biodeterior. Biodegradation. 124 (2017) 196–205. doi:10.1016/j.ibiod.2017.06.013.

[26] APHA/AWWA/WEF, Standard methods for the examination of water and wastewater, twentieth ed., American Public Health Association/American Water Works Association/Water Environment Federation, Washington D.C., 1999.

[27] D. Villa-Gomez, H. Ababneh, S. Papirio, D.P.L. Rousseau, P.N.L. Lens, Effect of sulfide concentration on the location of the metal precipitates in inversed fluidized bed reactors, J. Hazard. Mater. 192 (2011) 200–207. doi:10.1016/j.jhazmat.2011.05.002.

[28] R. Khanongnuch, F. Di Capua, A.-M. Lakaniemi, E.R. Rene, P.N.L. Lens, Effect of N/S ratio on anoxic thiosulfate oxidation in a fluidized bed reactor: experimental and

artificial neural network model analysis, Process Biochem. 68 (2018) 171–181. doi:https://doi.org/10.1016/j.procbio.2018.02.018.

[29] C. Kennes, E.R. Rene, M.C. Veiga, Bioprocesses for air pollution control, J. Chem. Technol. Biotechnol. 84 (2009) 1419–1436. doi:10.1002/jctb.2216.

[30] G. Soreanu, M. Béland, P. Falletta, K. Edmonson, P. Seto, Laboratory pilot scale study for H_2S removal from biogas in an anoxic biotrickling filter, Water Sci. Technol. 57 (2008) 201–207. doi:10.2166/wst.2008.023.

[31] J. Brito, F. Almenglo, M. Ramírez, J.M. Gómez, D. Cantero, PID control system for biogas desulfurization under anoxic conditions, J. Chem. Technol. Biotechnol. 92 (2017) 2369–2375. doi:10.1002/jctb.5243.

[32] F. Di Capua, S.H. Ahoranta, S. Papirio, P.N.L. Lens, G. Esposito, Impacts of sulfur source and temperature on sulfur-driven denitrification by pure and mixed cultures of *Thiobacillus*, Process Biochem. 51 (2016) 1576–1584. doi:10.1016/j.procbio.2016.06.010.

[33] Y. Wang, S. Zhou, H. Wang, L. Ye, J. Qin, X. Lin, Comparison of endogenous metabolism during long-term anaerobic starvation of nitrite/nitrate cultivated denitrifying phosphorus removal sludges, Water Res. 68 (2015) 374–386. doi:10.1016/j.watres.2014.09.044.

[34] C. Jing, Z. Ping, Q. Mahmood, Simultaneous sulfide and nitrate removal in anaerobic reactor under shock loading, Bioresour. Technol. 100 (2009) 3010–3014. doi:10.1016/j.biortech.2008.12.041.

[35] L.R. López, J. Brito, M. Mora, F. Almenglo, J.A. Baeza, M. Ramírez, J. Lafuente, D. Cantero, D. Gabriel, Feedforward control application in aerobic and anoxic biotrickling filters for H_2S removal from biogas, J. Chem. Technol. Biotechnol. 93 (2018) 2307–2315. doi:DOI 10.1002/jctb.5575.

[36] H. Satoh, M. Odagiri, T. Ito, S. Okabe, Microbial community structures and in situ sulfate-reducing and sulfur-oxidizing activities in biofilms developed on mortar specimens in a corroded sewer system, Water Res. 43 (2009) 4729–4739. doi:10.1016/j.watres.2009.07.035.

[37] E. Cardenas, W.-M. Wu, B.M. Leigh, J. Carley, S. Carroll, T. Gentry, J. Luo, D. Watson, B. Gu, M. V. Ginder-Vogel, P.K. Kitanidis, P.M. Jardine, J. Zhou, C.S. Criddle, T.L. Marsh, J.M. Tiedje, Significant association between sulfate-reducing bacteria and uranium-reducing microbial communities as revealed by a combined massively parallel sequencing-indicator species approach, Appl. Environ. Microbiol. 76 (2010) 6778–6786. doi:10.1128/AEM.01097-10.

[38] L. Lu, C. Zeng, L. Wang, X. Yin, S. Jin, A. Lu, Z. Jason Ren, Graphene oxide and H_2 production from bioelectrochemical graphite oxidation, Sci. Rep. 5 (2015) 16242. doi:10.1038/srep16242.

List of figure captions

Fig. 1. Effect of different liquid flow rates (a) on the BTF performance (phase I): loading rate and elimination capacity of NO_3^- and N/S ratio (b), inlet and outlet H_2S and SO_4^{2-} production rate (c), and influent and effluent pH profiles (d).

Fig. 2. BTF performance during 12 h wet-12 h dry operation (phase II): inlet and outlet H_2S (a), SO_4^{2-} production rate (b) and influent and effluent NO_3^- and NO_2^- (c).

Fig. 3. BTF performance during 24 h wet-24 h dry operation (phase II): inlet and outlet H_2S (a), SO_4^{2-} production rate (b) and influent and effluent NO_3^- and NO_2^- (c).

Fig. 4. BTF performance during 1 h wet-1 h dry and 2 h wet-2 h dry operations (phase II): inlet and outlet H_2S (a), SO_4^{2-} production rate (b) and influent and effluent NO_3^- and NO_2^- (c).

Fig. 5. H_2S elimination capacity of the anoxic BTF under different transient-state operations tested in this study: wet-dry bed operations (a) and H_2S shock loads and bioaugmentation (b).

Fig. 6. BTF performance under the influence of different H_2S shock loads (phase III): inlet and outlet H_2S (a), SO_4^{2-} production rate (b) and influent and effluent NO_3^- and NO_2^- (c).

Fig. 7. Effect of bioaugmentation with a facultative autotrophic biomass dominated by *Paracoccus* MAL 1HM19 on the BTF performance (phase IV): inlet and outlet H_2S (a), SO_4^{2-} production rate (b) and influent and effluent NO_3^- and NO_2^- (c).

Fig. 8. Microbial community profiles (left) and identification of the sequenced denaturing gradient gel electrophoresis bands (right) of the biomass samples collected before (day 0), after transient-state conditions (day 62) and bioaugmentation (day 78). Each sample was run in duplicate.

Table 1. Transient-state operation of the anoxic biotrickling filter (BTF) for the simultaneous removal of H_2S and NO_3^-.

	Specific experiments	Inlet H_2S concentration (ppm_v)	H_2S loading rate (g S m^{-3} h^{-1})	Gas flow rate (L h^{-1})	EBRT[b] (min)	NO_3^- loading rate (g NO_3^--N m^{-3} h^{-1})	Liquid flow rate (L d^{-1})	Operational days	Days of normal conditions[a]
	Normal conditions[a]	116 (±2)	4.3 (±0.1)	60	3	3.8 (±0.1)	60	-	-
I	Effect of liquid flow rate	98 (±8)	3.7 (±0.3)	60	3	2.7-11.3	30, 60 and 120	0-21	20-21
II	Effect of wet-dry bed operations	109 (±12)	4.2 (±0.4)	60	3	4.0 (±0.1)	60		
	(i) 12 h wet-12 h dry							22-30	29-30
	(ii) 24 h wet-24 h dry							31-41	40-41
	(iii) 1 h wet-1 h dry							42-45	43-45
	(iv) 2 h wet-2 h dry							46-50	48-50
III	Effect of H_2S shock loads:								
	(i) increasing the gas flow rate	115 (±18)	4.4 (±0.8) and 14.0 (±1.5)	60 and 200	3 and 0.9	3.8 (±0.2)	60	51-55	54-55
	(ii) increasing the H_2S concentration	112 (±15) and 947 (±151)	4.2 (±0.6) and 35.5 (±5.6)	60	3	3.9 (±0.2)	60	56-62	58, 61-62
IV	Bioaugmentation with *Paracoccus* MAL 1HM19 followed by the H_2S shock load test	110 (±13) and 982 (±70)	4.1 (±0.4) and 36.8 (±2.6)	60	3	3.8-16.6	60	63-78	-

Note: [a] Normal operation was applied for stabilizing/recovering the H_2S RE of the BTF at the end of each transient-state tests.
[b] EBRT = empty bed residence time of the gas phase H_2S.

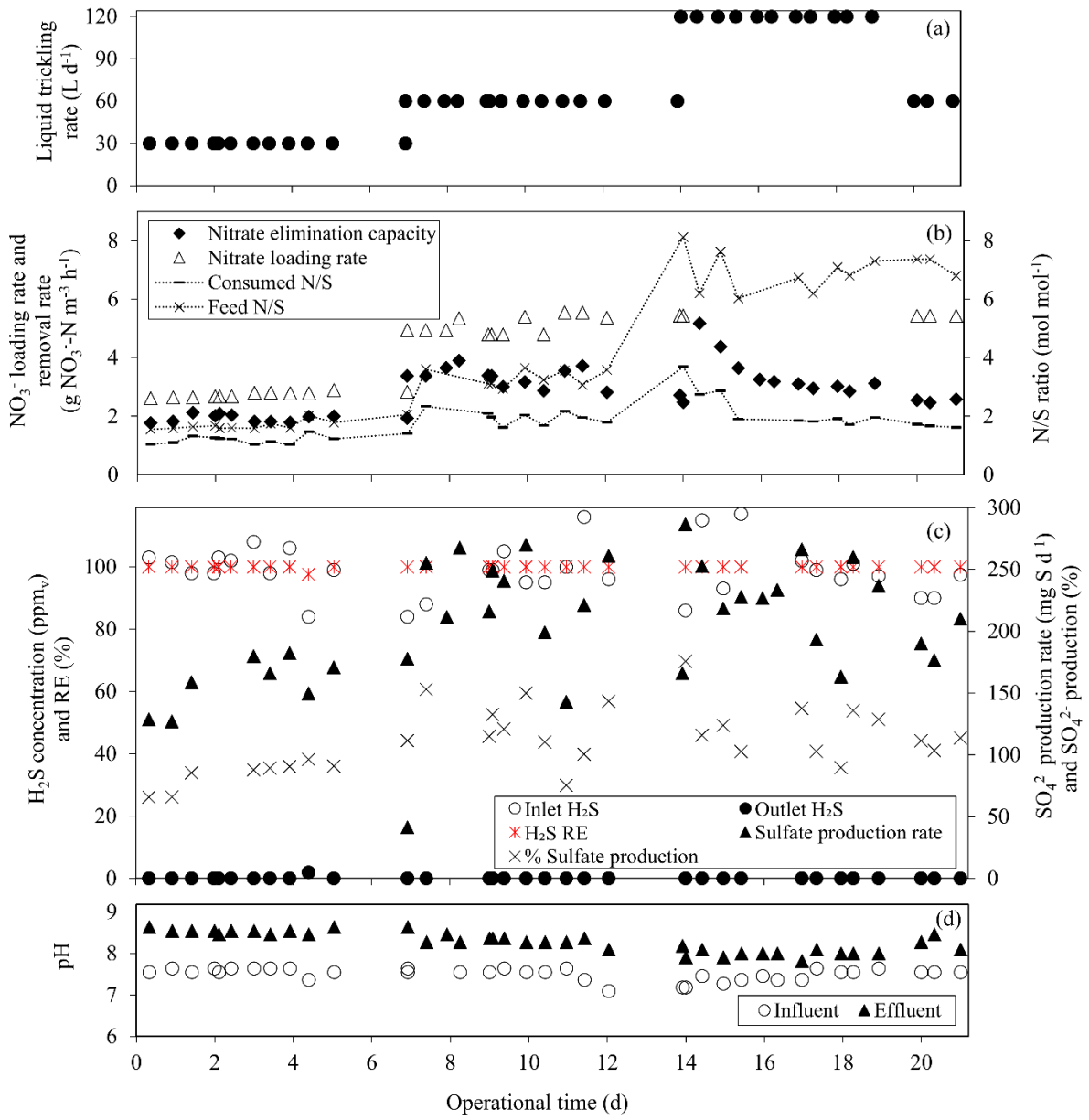
(a)
Liquid trickling rate (L d-1)
(b)
Nitrate elimination capacity
Nitrate loading rate
Consumed N/S
Feed N/S
NO3- loading rate and removal rate (g NO3--N m-3 h-1)
N/S ratio (mol mol-1)
(c)
H2S concentration (ppmv) and RE (%)
SO42- production rate (mg S d-1) and SO42- production (%)
Inlet H2S
Outlet H2S
H2S RE
Sulfate production rate
% Sulfate production
(d)
pH
Influent
Effluent
Operational time (d)

Fig. 1.

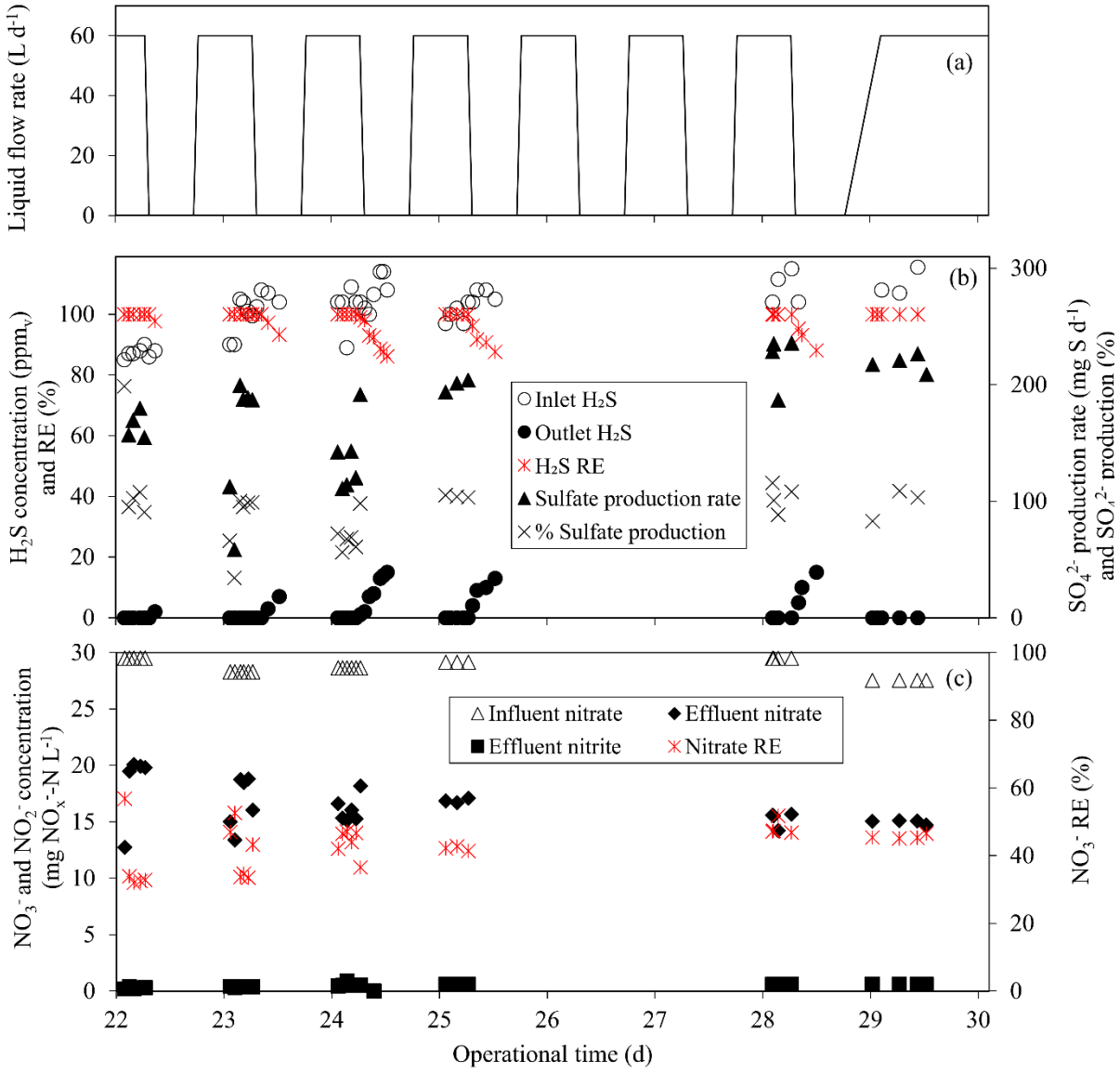
Liquid flow rate (L d-1)
(a)
H2S concentration (ppmv) and RE (%)
(b)
SO4 2- production rate (mg S d-1) and SO4 2- production (%)
Inlet H2S
Outlet H2S
H2S RE
Sulfate production rate
% Sulfate production
NO3- and NO2- concentration (mg NOx-N L-1)
(c)
NO3- RE (%)
Influent nitrate
Effluent nitrate
Effluent nitrite
Nitrate RE
Operational time (d)

Fig. 2.

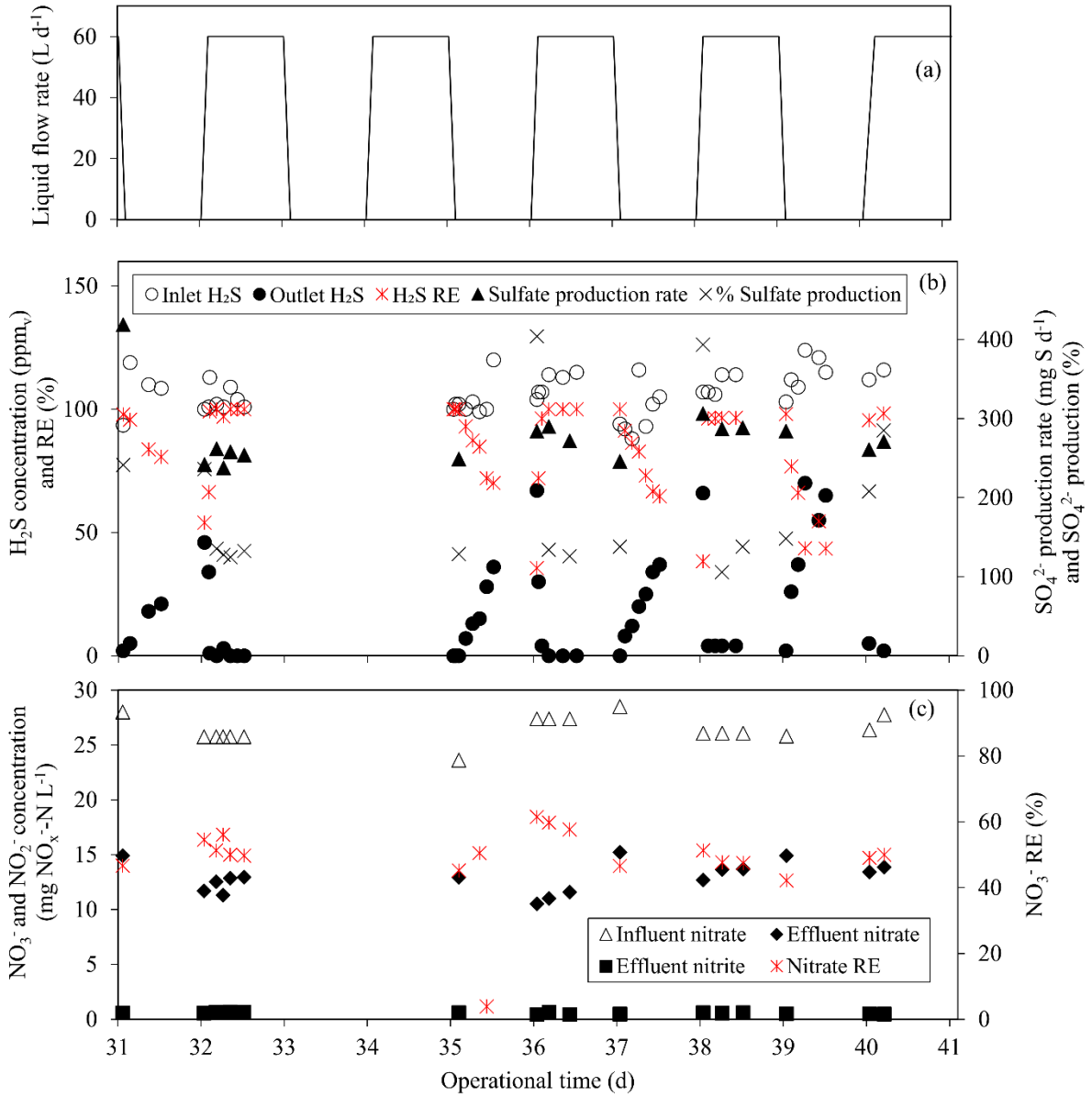
Liquid flow rate (L d-1)
(a)
H2S concentration (ppmv) and RE (%)
Inlet H2S
Outlet H2S
H2S RE
Sulfate production rate
% Sulfate production
(b)
SO4 2- production rate (mg S d-1) and SO4 2- production (%)
NO3- and NO2- concentration (mg NOx-N L-1)
(c)
Influent nitrate
Effluent nitrate
Effluent nitrite
Nitrate RE
NO3- RE (%)
Operational time (d)

Fig. 3

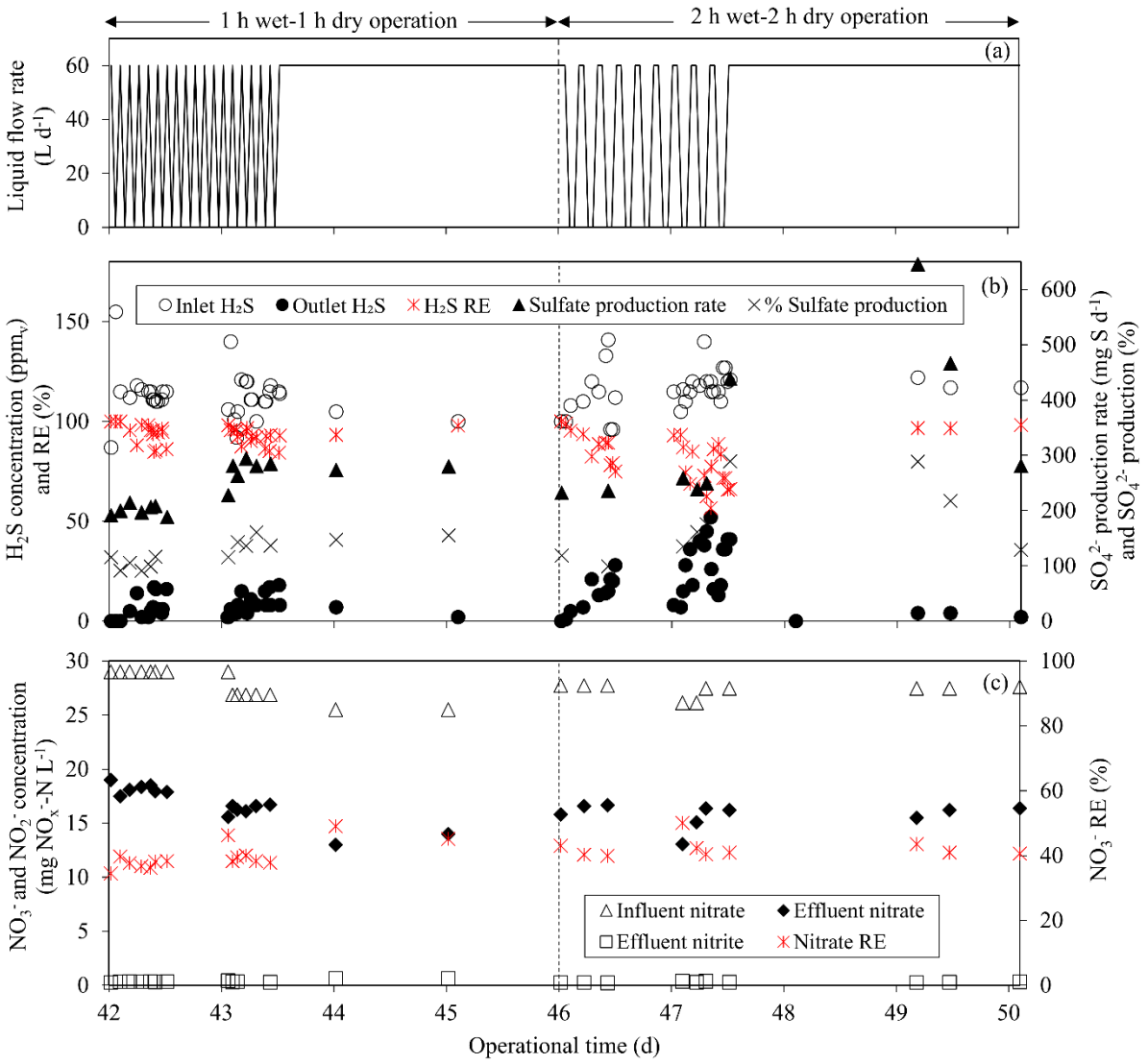
1 h wet-1 h dry operation
2 h wet-2 h dry operation
(a)
Liquid flow rate (L d-1)
(b)
Inlet H2S
Outlet H2S
H2S RE
Sulfate production rate
% Sulfate production
H2S concentration (ppmv) and RE (%)
SO4 2- production rate (mg S d-1) and SO4 2- production (%)
(c)
Influent nitrate
Effluent nitrate
Effluent nitrite
Nitrate RE
NO3- and NO2- concentration (mg NOx-N L-1)
NO3- RE (%)
Operational time (d)

Fig. 4.

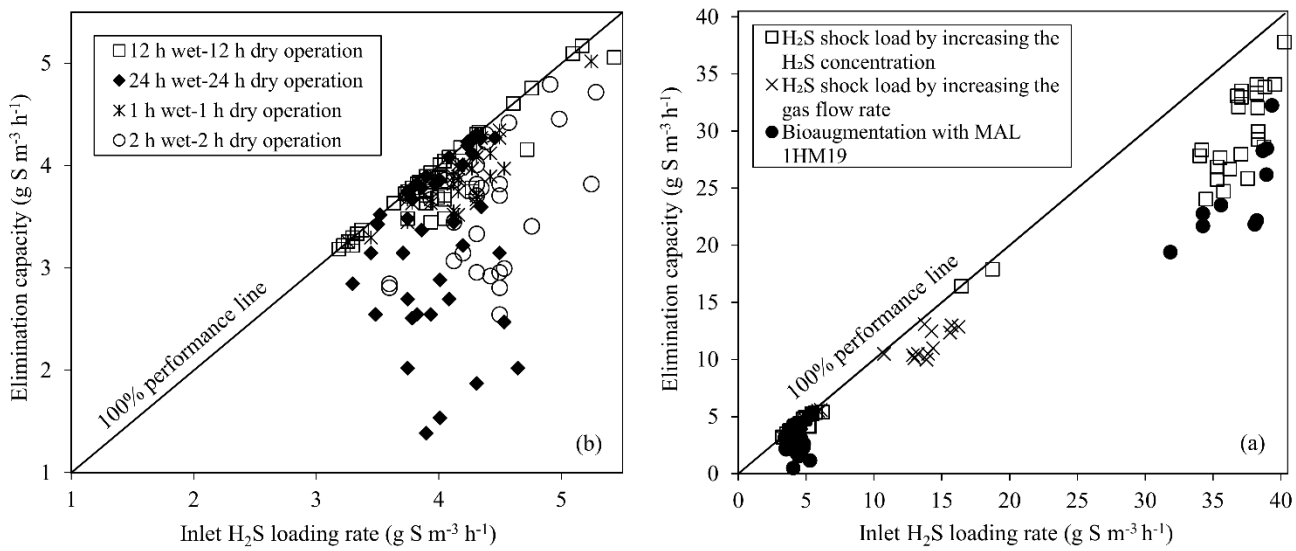
□12 h wet-12 h dry operation
◆24 h wet-24 h dry operation
✳1 h wet-1 h dry operation
○2 h wet-2 h dry operation
100% performance line
(b)
Elimination capacity (g S m-3 h-1)
Inlet H2S loading rate (g S m-3 h-1)
□H2S shock load by increasing the H2S concentration
×H2S shock load by increasing the gas flow rate
●Bioaugmentation with MAL 1HM19
100% performance line
(a)
Elimination capacity (g S m-3 h-1)
Inlet H2S loading rate (g S m-3 h-1)

Fig. 5.

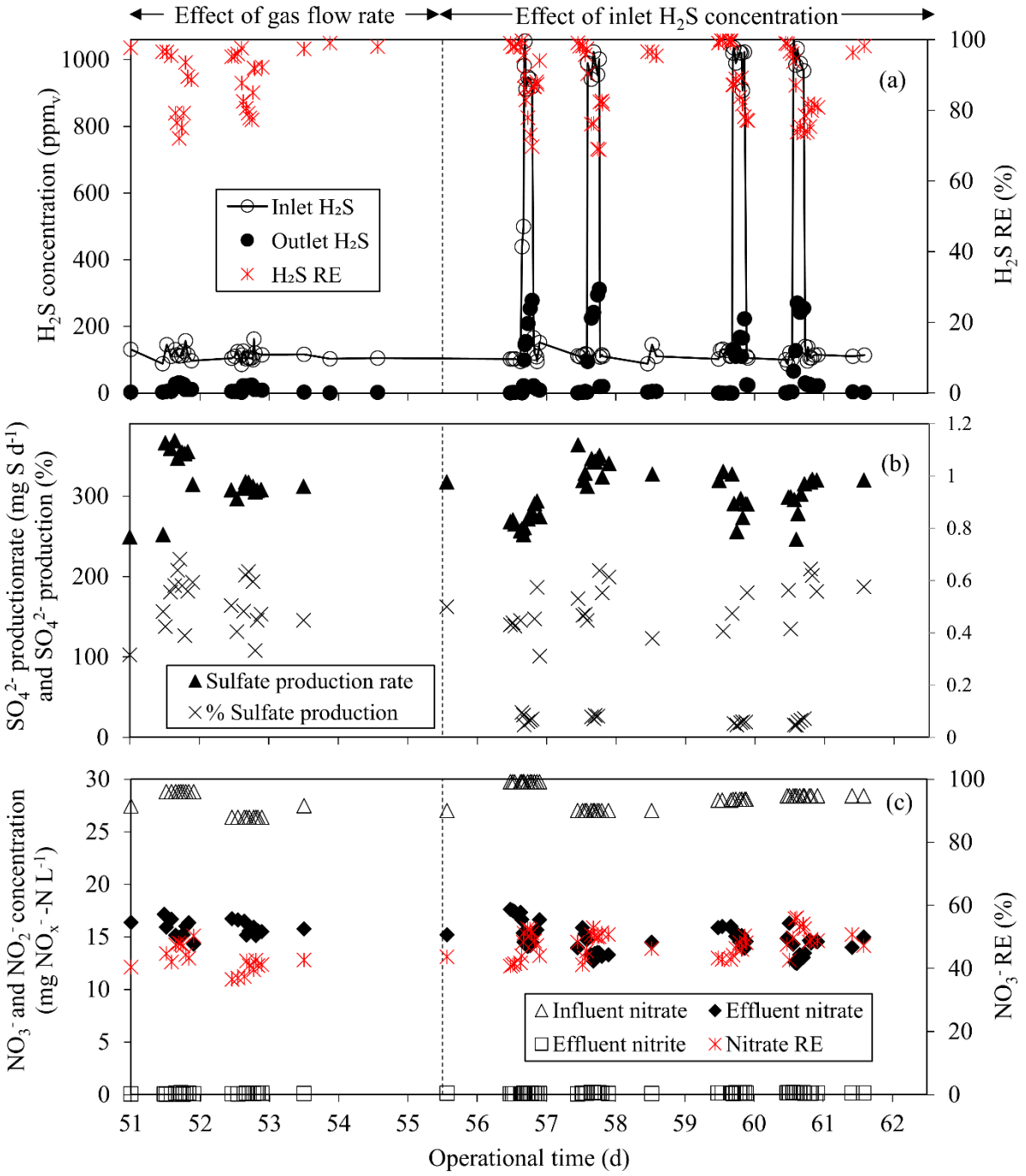
Effect of gas flow rate
Effect of inlet H2S concentration
(a)
H2S concentration (ppmv)
H2S RE (%)
Inlet H2S
Outlet H2S
H2S RE
(b)
SO4 2- productionrate (mg S d-1) and SO4 2- production (%)
Sulfate production rate
% Sulfate production
(c)
NO3 - and NO2 - concentration (mg NOx - -N L-1)
NO3 - RE (%)
Influent nitrate
Effluent nitrate
Effluent nitrite
Nitrate RE
Operational time (d)

Fig. 6.

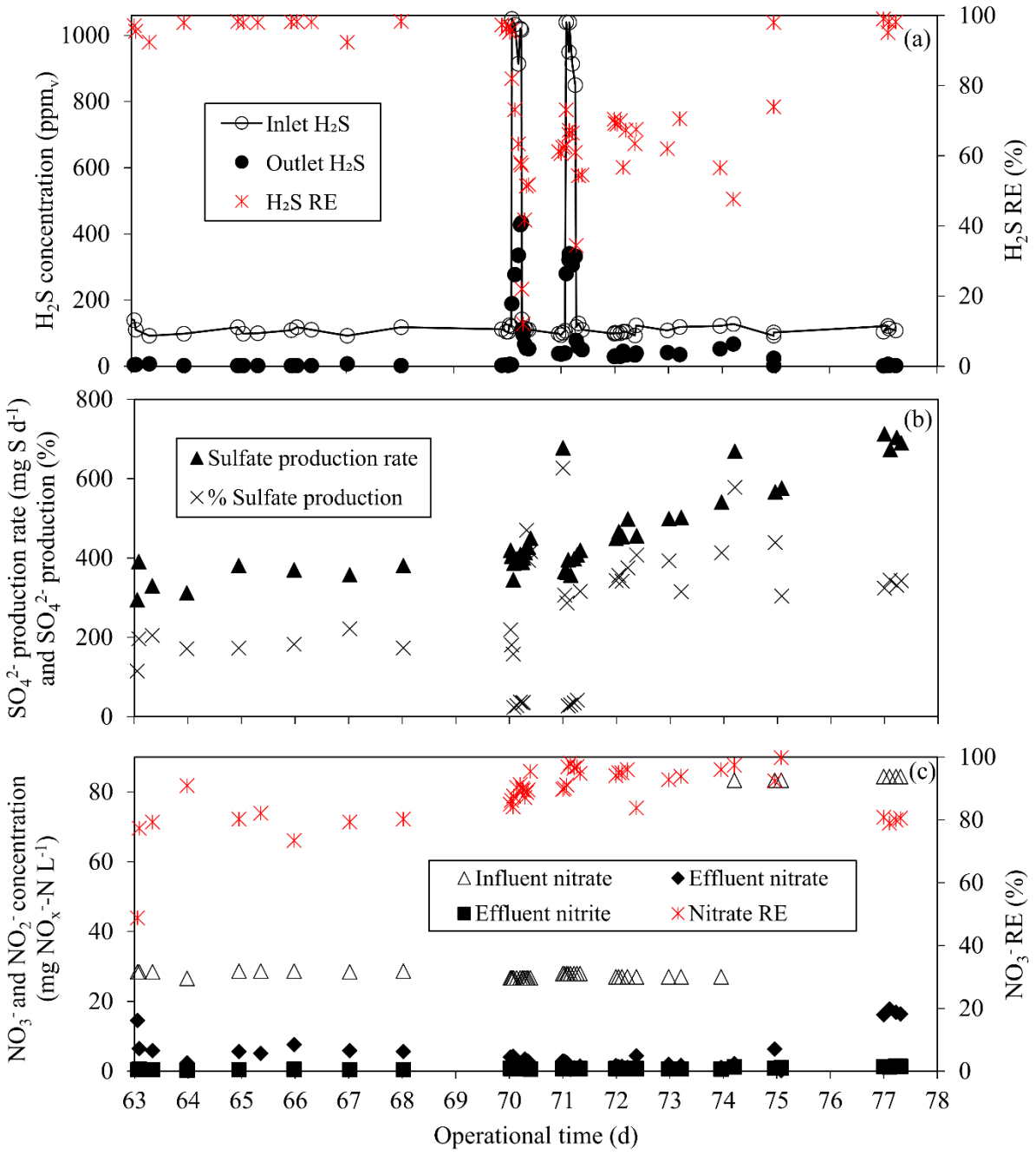
(a)
Inlet H2S
Outlet H2S
H2S RE
H2S concentration (ppmv)
H2S RE (%)
(b)
Sulfate production rate
% Sulfate production
SO4 2- production rate (mg S d-1) and SO4 2- production (%)
(c)
Influent nitrate
Effluent nitrate
Effluent nitrite
Nitrate RE
NO3- and NO2- concentration (mg NOx-N L-1)
NO3- RE (%)
Operational time (d)

Fig. 7.

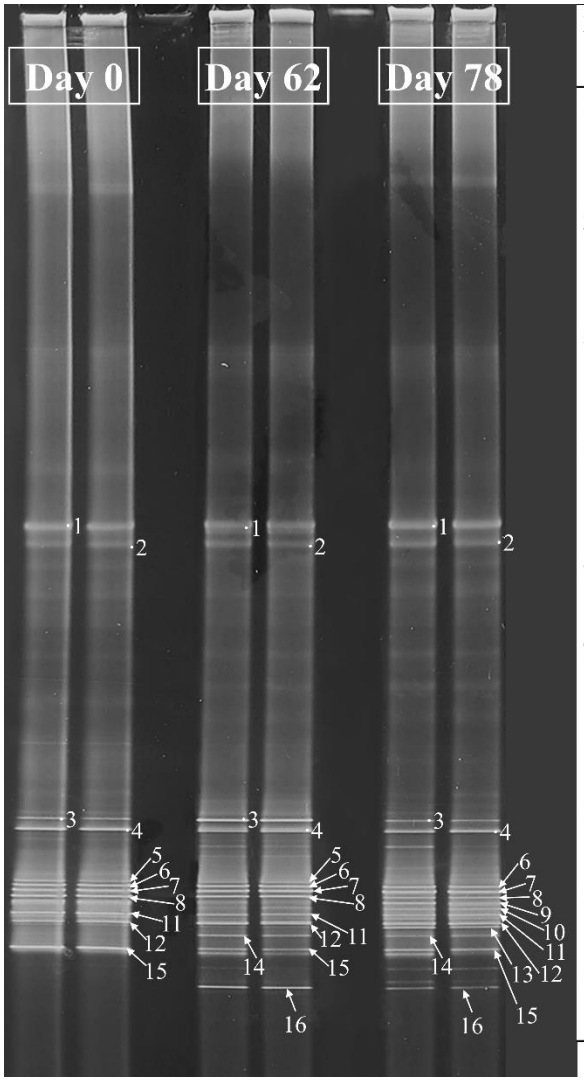

Band(s)[a]	Class/order/family	Affiliation[b]	Accession number	Similarity (%)	Sequence length
1, 11	γ -proteobacteria/Xanthomonadales/ Xanthomonadaceae	*Stenotrophomonas* sp.	KY490132.1, KM021209.1	91.8-94.5	456-510
2, 15	α-proteobacteria/Rhodobacterales/ Rhodobacteraceae	*Rhodobacter* sp.	LN879886.1, JN648234.1	92.6-99.1	415-429
3, 4	-	Bacteroidetes/Chlorobi group bacterium	KU685184.1, LN998004.1	96.2-96.3	416-418
5, 7, 8	β-proteobacteria/Nitrosomonadales/ Thiobacillaceae	*Thiobacillus* sp.	KM200026.1, JX530173.1, KM200014.1	98.0-100	433-508
6	β-proteobacteria/Rhodocyclales	*Rhodocyclales* bacterium	JQ723653.1, JQ723670.1	98.7	448
9	β-proteobacteria/Burkholderiales/ Comamonadaceae	*Simplicispira* sp.	KY476421.1	89.8	440
10, 13	α-proteobacteria/Rhodobacterales/ Rhodobacteraceae	*Paracoccus* sp.	KY427435.1	98.0	482
12	-	Uncultured β proteobacterium	EF667513.1	92.4	431
14	α-proteobacteria/Holosporales/ Holosporaceae	Endosymbiont of *Acanthamoeba* sp.	CP004403.1	99.1	430
16	δ-proteobacteria/Desulfuromonadales/ Geobacteraceae	*Geobacter* sp.	EF658628.1	99.3	433

Note: [a] Band label of DGGE-separated DNA fragments, and [b] Closet relative DGGE-separated DNA fragment in the GenBank

Fig. 8.